Multidisciplinary Preclinical Investigations on Three Oxamniquine Analogues as Novel Treatment Options for Schistosomiasis

Valentin Buchter, Yih Ching Ong, François Mouvet, Abdallah Ladaycia, Elise Lepeltier, Ursula Rothlisberger, Jennifer Keiser, Gilles Gasser

Multidisciplinary Preclinical Investigations on Three Oxamniquine Analogues as Novel Drug Candidates for Schistosomiasis

Valentin Buchter,[1,2,#] Yih Ching Ong,[3,#] François Mouvet,[4,#] Abdallah Ladaycia,[5] Elise Lepeltier,[5] Ursula Rothlisberger,[4,*] Jennifer Keiser,[1,2,*] and Gilles Gasser[3,*]

[1] Swiss Tropical and Public Health Institute, Socinstrasse 57, P.O. box, CH-4002 Basel, Switzerland.

[2] University of Basel, Petersplatz 1, P.O. Box, CH-4001 Basel, Switzerland.

[3] Chimie ParisTech, PSL University, CNRS, Institute of Chemistry for Life and Health Sciences, Laboratory of Inorganic Chemical Biology, F-75005 Paris, France.

[4] Laboratory of Computational Chemistry and Biochemistry, EPFL, 1015 Lausanne, Switzerland.

[5] MINT, UNIV Angers, INSERM 1066, CNRS 6021, Université Bretagne Loire, 4 rue Larrey, 49933 Angers Cedex 9, France.

ORCID

Valentin Buchter: 0000-0002-1985-0676

Yih Ching Ong: 0000-0003-0411-1114

François Mouvet 0000-0002-0416-2598

Abdallay Ladaycia: 0000-0003-3931-0498

Elise Lepeltier: 0000-0002-7666-6453

Ursula Rothlisberger 0000-0002-1704-8591

Jennifer Keiser: 0000-0003-0290-3521

Gilles Gasser: 0000-0002-4244-5097

Abstract

Schistosomiasis is a disease of poverty affecting millions of people. Praziquantel (PZQ), with its strengths and weaknesses, is the only treatment available. We previously reported findings on 3 lead compounds derived from oxamniquine (OXA), an old antischistosomal drug: ferrocene-containing (Fc-CH_2-OXA), ruthenocene-containing (Rc-CH_2-OXA) and benzene-containing (Ph-CH_2-OXA) OXA derivatives. These derivatives showed excellent *in vitro* activity against both *Schistosoma mansoni* larvae and adult worms and *S. haematobium* adult worms, and *in vivo* activity against *S. mansoni*. Encouraged by these promising results, we conducted additional in-depth preclinical studies and report in this investigation on metabolic stability studies, *in vivo* studies on *S. haematobium* and juvenile *S. mansoni*, computational simulations, and formulation development. Molecular dynamics simulations supported the *in vitro* results on the target protein. Though all three compounds were poorly stable within an acidic environment, they were only slightly cleared in the *in vitro* liver model. This is likely the reason as to why the promising *in vitro* activity did not translate to *in vivo* activity on *S. haematobium*. This limitation could not be saved by the formulation of lipid nanocapsules as an intent to improve the *in vivo* activity. Further studies should focus on increasing the compound's bioavailability, in order to reach an active concentration in the parasite's microenvironment.

Keywords: Bioorganometallic Chemistry; Molecular Dynamics; Medicinal Organometallic Chemistry; Metabolic Stability; Schistosomiasis.

Introduction

S. mansoni, S. haematobium and *S. japonicum* account for over 90% of the cases of schistosomiasis, an acute and chronic parasitic disease that affects over 200 million people worldwide[1-3] and threatens more than 700 million people the risk of infection.[4] In children, schistosomiasis stunts physical growth and ability to learn, while in adults, the disease affects the ability to work, and can cause organ failure and ultimately death, a situation that causes an enormous socioeconomic burden for developing communities.[5] Praziquantel (PZQ) is the only drug being used for periodic mass drug administration to control the disease. Considering the threatening and real possibility of resistance[6] and that PZQ presents drawbacks, our efforts are oriented to identify and develop a new molecule with the potential to become an alternative therapeutic option in the treatment of this disease.

Oxamniquine (OXA, Figure 1) is an anthelmintic drug developed in the 1960s[7] that showed high activity and a very convenient drug profile in terms of safety and ease of administration. It became the cornerstone of the schistosomiasis eradication program in Brazil in the past and beginning of the 21st centuries but fell into disuse because of two main reasons: it was only active against adult *S. mansoni*[7-9] and resistance was clinically confirmed. The drug was therefore no longer commercialized after 2010 and replaced by PZQ.[7] OXA is a prodrug that needs to be activated by the sulfotransferase of *S. mansoni* (SmULT) to an alkylating molecule that binds proteins and DNA, consequently killing the parasite.[10] Different enzyme orthologues are present in all S*chistosoma* species, but only the active site of the sulfotransferase of *S. mansoni* can activate OXA.[11]

OXA was administered as a 1:1 racemate mixture, with both enantiomers having anti-parasitic activity, although the S-OXA contributes the most. Crystal structures of R-OXA and S-OXA complexes with SmSULT target show similarities in the modes of OXA binding, but only the S-OXA enantiomer is observed in the structure of the enzyme exposed to racemic OXA[12].

The mechanism of resistance and lack of activity in the remaining species has been well studied. Resistance is based in one or more point mutations in the enzyme's active site that prevent the molecule to be sulfonated.[13] Taking into account that there is a 70% homology between the amino acid sequences of the sulfotransferases of *S. mansoni* and *S. haematobium*,[11] we derivatized OXA based on the hypothesis that modification of OXA could overcome the species and stage specificity. [14]

Previous studies by Jaouen and co-workers on the anticancer drug candidate ferrocifen[15-17] and Brocard, Biot and co-workers on the anti-malarial drug candidate ferroquine showed that the ferrocenyl analogues of tamoxifen and chloroquine, respectively have improved bioactivity compared to the original organic drug compounds.[18, 19] This was due to several factors: the ferrocenyl component acted as a producer of reactive oxygen species (ROS), increased the lipophilic character of the molecule and provided a mechanism of action different to that of the original drug.[20-22] With this concept in mind, we developed several metal-containing derivatives of OXA, which were studied *in vitro* and *in vivo* against *Schistosoma spp.* [23-25] Among others, we demonstrated that the three derivatives of OXA, namely a ferrocene- (Fc-CH_2-OXA), ruthenocene- (Rc-CH_2-OXA) and benzene-containing (Ph-CH_2-OXA) derivative (Figure 1), showed promising *in vitro* results, where all three OXA derivatives caused death of *S. mansoni* and *S. haematobium* adult worms[25] and worm burden reductions of 76 to 93% against adult *S. mansoni in vivo.*[23]Encouraged by our promising preliminary results, we decided to go further in the development and to fully characterize these three OXA analogues. *In vitro* studies were conducted against *S. mansoni* juvenile worms, and *S. japonicum* and *S. haematobium* adult worms. *In vivo* studies were carried out against adult *S. haematobium* and juvenile *S. mansoni* including studies with Ph-CH_2-OXA encapsulated in Lipid NanoCapsules (LNC). Only racemic mixtures were tested

as we focused on determining the presence of activity for the OXA derivatives *in vivo* with *S. mansoni* and *S. haematobium*, rather than spending time on isolating the enantiomers if these compounds were not active. Stability in acidic conditions are also determined as the final goal to develop these derivatives as orally administered compounds which pass through the stomach's acidic environment. Our work was complemented by computational models and molecular dynamics simulations as well as microsomal stability and albumin binding studies.

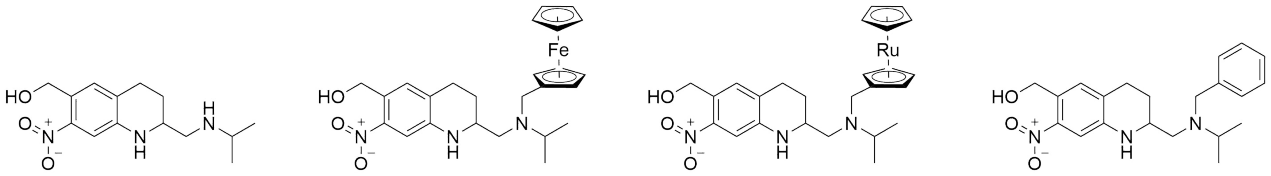

Figure 1. Structures of the compounds investigated in this study.

Results and Discussion

***In vitro* studies**

Fc-CH_2-OXA, Rc-CH_2-OXA and Ph-CH_2-OXA previously demonstrated promising activity as drug candidates *in vitro* against adult *S. mansoni* and S. *haematobium* and first stage of the larval development (NTS: newly transformed schistosomula) and *in vivo* in adult *S. mansoni* infected mice.[23, 25] In order to test the full potential of our compounds, we first elucidated the *in vitro* activity of the OXA derivatives against 28-day-old juvenile *S. mansoni* worms since one of the important drawbacks of PZQ is its low activity against this developmental stage. All three compounds killed all the worms within 24 h of incubation at a concentration of 100 µM (Table 1). Against juvenile *S. mansoni*, Fc-CH_2-OXA had the lowest IC_{50} (0.5 µM) while Ph-CH_2-OXA was the drug with the highest IC_{50} value (26.7 µM), the one with the lowest activity. Interestingly, in the case of Ph-CH_2-OXA, the effect of the molecules on the juveniles was faster than against the adults: while on adult *S. mansoni,* Ph-CH_2-OXA needed 72 h to exert its maximal activity; against juvenile

stages, we observed a total lethal effect within 24 h of incubation at a dose of 100 µM. For comparison, by the same incubation time, juvenile *S. mansoni* exposed to OXA showed an IC_{50} of >100 µM, confirming previous studies of OXA being only slightly active *in vitro* and against juvenile stages of the parasite.[9, 25] Only by 72 h of incubation at 100 µM, where the derivatives had long exerted their activity, we found a 48% reduction of the viability of OXA respect to the control worms (Table S2).

Against *S. japonicum* adult worms, we observed the same behavior: while OXA was not active even by 100 µM after 3 days (Table 1 and Table S2), our derivatives showed considerable activity. Of the three derivatives tested, Fc-CH_2-OXA proved to be the most active of all three derivatives, killing all the parasites within 24 h at a concentration of 100 µM and having the lowest IC_{50} value (22.6 µM). On *S. haematobium* instead, the most active compound was Rc-CH_2-OXA, also killing all parasites at a concentration of 100 µM and revealing the lowest IC_{50} value (15.5 µM).

Moreover, we incubated adult *S. mansoni* in medium containing albumin and compared the activity determined to our standard assay. A lower activity of the three drugs was observed in the enriched medium, with Fc-CH_2-OXA showing the least loss of activity of the three derivatives (Table 1). The albumin binding experiment was also performed for adult *S. haematobium.* Also in this case, the three compounds showed a reduction of the activity. These results are comparable with those obtained by Pasche *et al,*[26] who also identified a significant decrease in drug activity incubating antischistosomal drug candidates *in vitro* in the presence of albumin. Also, PZQ presents a high percentage (around 80%) of drug bound to protein[27] and this might be one of the reasons for the high doses needed to reach a significant effect. Protein binding is a major issue in drug development, since only the free fraction of the drug is able to interact with the target.[28]

Table 1. *In vitro* activity of Fc-CH_2-OXA, Rc-CH_2-OXA and Ph-CH_2-OXA versus OXA against *S. mansoni*, *S. haematobium* and *S. japonicum*.

Compound	*S. mansoni*				*S. haematobium*		*S. japonicum*
	IC_{50} adults 72 h (µM)	**IC_{50} adults in medium 45 g/L albumin. 72 h (µM)**	**Onset of action on juveniles 100 µM (h)**	**IC_{50} 28 day juveniles 72 h (µM)**	**IC_{50} adults 72 h (µM)**	**IC_{50} adults in medium with albumin. 72 h (µM)**	**IC_{50} adults 72 h (µM)**
Fc-CH_2-OXA	9.0	28.1	< 24	0.5	52.3	55.7	22.7
Rc-CH_2-OXA	6.0	NC	< 24	1.3	15.5	25	30.9
Ph-CH_2-OXA	13.5	90.7	< 24	26.7	32.6	70.6	39.8
OXA	>100	>100	72	>100	>100 *	ND	>100

* Hess et al.[23] , NC: no correlation, ND: not done.

Studies on juvenile *S. mansoni* in the mouse model

In terms of activity against juvenile parasites *in vivo*, we identified a lower activity of all three compounds in respect to the results on adult parasites.[23] Though the drug showed moderate activity, as shown by their shift to the liver due to the loss of vein attachment (data not shown), worm burden reductions were low ranging from 39 to 47% (Table 2).When considering the gender of the surviving worms we evidence that there is no gender difference in susceptibility (binomial test, $p > 0.77$).

Table 2: Reduction of the juvenile worm burden in *S. mansoni* infected mice after treatment with 200 mg/kg of the OXA derivatives and after treatment with the nano encapsulated Ph-CH_2-OXA.

Compound	No. of mice	Worm burden (SD)		WBR % pure drug (SD)		WBR % nanocapsule	
		Females	**Total**	**Females**	**Total**	**Females**	**Total**
Control group	8	6.5 (1.6)	12.3 (2.5)	-	-		
Fc-CH_2-OXA	4	3.8 (0.96)	7.5 (2.65)	42.3 (14.7)	38.8 (21.6)	ND	ND
Rc-CH_2-OXA	4	3 (2.45)	6.5 (4.43)	53.8 (7.7)	46.9 (36.2)	ND	ND
Ph-CH_2-OXA	4	4.3 (0.5)	7.5 (0.58)*	34.6 (7.7)	38.8 (4.7)*	0	0

ND: Not done; WBR: worm burden reduction. *Statistically different from control on $p<0.05$

In vivo* studies on adult *S. haematobium

Table 3 shows the worm burden reduction of the three compounds against *S. haematobium*: none of the compounds affected *S. haematobium in vivo,* contradicting the findings observed *in vitro*.

Table 3: Change in the worm burden of *S. haematobium* infected hamsters after treatment with 200 mg/kg of the OXA derivatives.

Compound	No. of mice	Worm burden (SD)		WBR %
		Females	Total	
Control group	4	18.5 (8.3)	40 (13.6)	-
Fc-CH_2-OXA	4	25.8 (7.5)	54 (16.2)	0
Rc-CH_2-OXA	3*	55 (16.1)	108 (28.9)	0
Ph-CH_2-OXA	4	19 (3.7)	51 (18.9)	0

*One animal died during the experiment.

Computational studies

In order to understand the interaction between OXA analogues and the sulfotransferase proteins from *S. mansoni* (SmSULT) and *S. haematobium* (ShSULT), we performed classical molecular dynamics simulations of OXA, Fc-CH_2-OXA, Ph-CH_2-OXA and Fc-CO-OXA to determine their binding poses within the active site of the two sulfotransferases at body temperature. Fc-CO-OXA was added to the comparison to include the case of a derivative that was shown to be less active against *S. mansoni in vitro* than the other compounds considered in the present study.[23]

We did not consider Rc-CH2-OXA explicitly since both from a geometrical and electrostatic point of view, the force field models for ferrocenyl and ruthenocenyl compounds are very similar and would likely yield comparable behavior at this simplified level of theory.

The free energy difference between bound and unbound states of a receptor-ligand complex is a direct measure of the binding affinity. To estimate this quantity from our trajectories, we used the MM/PBSA (Table 4) and MM/GBSA methods (Table S1). All binding free energies are negative, meaning that the bound state is energetically favorable for all compounds. No systematic difference can be noted between the two proteins and all modified OXA compounds show a higher binding affinity than OXA itself. This is probably due to their larger size, forcing a tighter fit inside

the protein and increasing the number of interactions with the binding pocket. Consequently, all analogues are strongly bound to their target proteins.

Table 4. Estimated binding free energies computed by the MM/PBSA method (kcal/mol).

Compound	*S. mansoni*		*S. haematobium*	
	R	***S***	***R***	***S***
Fc-CH_2-OXA	-39.3	-41.9	-36.3	-39.9
Fc-CO-OXA	-36.3	-29.9	-26.4	-32
Ph-CH_2-OXA	-30.3	-35	-36.6	-18.3
OXA	-12.5	-8	-17.1	-22.8

Since the drugs are supposed to react with PAPS within the target protein, the distance between the closest oxygen of the sulfate group of PAPS and the hydrogen in the hydroxyl group of each drug was measured every 40 ps. These distances are represented as histograms in Figure 2 and their average is shown in Table 5. The near-attack configurations (NAC), i.e., the ones with shorter distances between the reactive groups are more likely to result in the activation of the compounds.

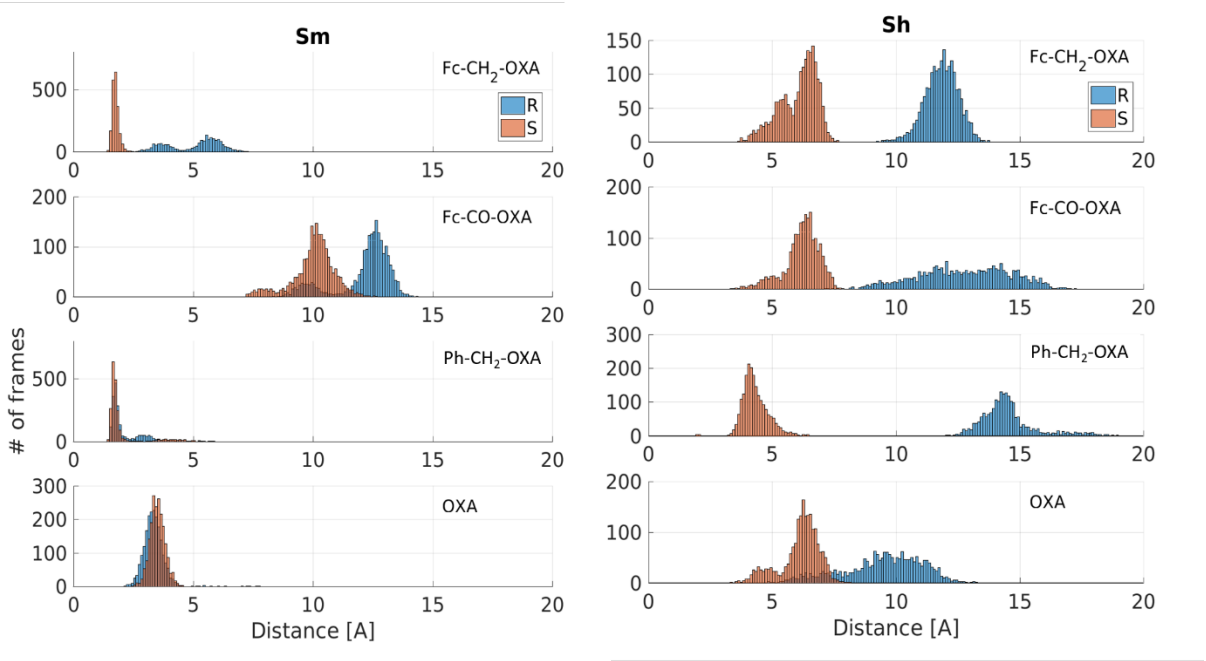

Figure 2. Distance between the closest oxygen of PAPS and the hydroxyl group of the analogues. *R*-enantiomers in blue and *S*-enantiomers in orange.

Table 5. Average O-H distance with standard deviation (Å)

Compound	*S. mansoni*		*S. haematobium*	
	R	***S***	***R***	***S***
Fc-CH_2-OXA	5.1 ± 1.1	1.8 ± 0.1	11.8 ± 0.7	6.1 ± 0.8
Fc-CO-OXA	12.2 ± 1.2	10.0 ± 0.9	12.8 ± 1.9	6.2 ± 0.7
Ph-CH_2-OXA	2.2 ± 0.7	2.0 ± 0.7	14.5 ± 1.1	4.3 ± 0.5
OXA	3.3 ± 0.4	3.5 ± 0.3	9.5 ± 1.6	6.1 ± 0.8

For OXA in SmSULT, the sulfate-hydroxyl distance is short and stable for both enantiomers, with an average slightly above 3 Å. The relative orientation of the reactive groups is fixed through their mutual interaction with ASN230, thus promoting the interaction (Figure S2). The chain of residues 19 to 23 also binds to PAPS and OXA at different places, stabilizing the configuration. For OXA, the difference between *R*- and *S*-enantiomers is very small, which is consistent with previous experimental works that already reported that both enantiomers bind in a similar fashion and that the activity difference originates from their binding kinetics.[12]

Both enantiomers of Ph-CH_2-OXA and Fc-CH_2-OXA show a very strong interaction with PAPS within SmSULT. Residues 18 to 21 bind both ligands in several places, highly stabilizing their binding (Figures S4 and S6). Moreover, the residue ASN230 also binds to PAPS and to the chain of residues 18-21, further increasing the stability. This may explain the high activity of these compounds *in vitro*. On the other hand, the *R*-enantiomer of Fc-CH_2-OXA seems to drift slowly away from PAPS and a proper equilibrium is never reached within our simulation time. The distance increases over time, which suggests that the final configuration will not be active. Strikingly, Ph-CH_2-OXA does not seem to be impacted by the enantiomer selectivity observed for all other derivatives.

Fc-CH_2-OXA, that was the most active against *S. mansoni* according to the *in vitro* experimental studies, shows short average distance to PAPS. In *S. haematobium* instead, the shortest distance to PAPS is held by the *S*-enantiomer of Ph-CH_2-OXA, which also shows a lower IC_{50} against this

species when compared to Fc-CH_2-OXA. Furthermore, our simulations of Fc-CO-OXA in SmSULT show NAC distributions where the reactants are about 3 times more distant than in OXA, with averages above 10 Å. These configurations are very unlikely to activate the drug, which is again consistent with experimental results.

In practice, OXA is not active on *S. haematobium*. In simulations where OXA is docked into ShSULT, we observe that the distance between the reactive groups is much larger than in SmSULT, by more than 6 Å on average. Furthermore, we observe a large difference between enantiomers, where the *R*-enantiomer shows a broad distribution of NAC distances with an average of 9.5 Å. This strong enantiomer dependence is present for all compounds and is more pronounced than in SmSULT with all *R*-enantiomers adopting less reactive configurations. The residue ASP80 seems to have a negative impact, forming a stable bond with the drug's hydroxyl group (Figures S3, S5, S7). This bond is far from PAPS, leading to unreactive geometries shown by a widening of the distance distributions between the compounds and PAPS. This residue is conserved in SmSULT, but stays at larger distances (more than 4.5 Å from the hydroxyl group of all considered compounds).

In ShSULT, the *S*-enantiomer of Ph-CH_2-OXA shows the most promising results. Our *in vitro* experiments showed that this compound was active against *S. haematobium* and our structures show significant improvements over OXA. The distances between reactant groups are significantly smaller, at about 4.3 Å on average and only slightly larger than for OXA in SmSULT, indicating that the compound could be activated. We also noticed that the difference between enantiomers is much larger in ShSULT than in SmSULT, suggesting that using enantiopure samples of Ph-CH_2-OXA instead of a racemic mixture may significantly improve the drug's efficacy against *S. haematobium.* However, given the overall low activity of the racemate *in vivo*, this specific point was not further evaluated.

Stability of OXA Analogues in Acidic Environments and in the Presence of Microsomes

We further investigated if the limited *in vivo* activity on juvenile *S. mansoni* and adult *S. haematobium* could be explained by physiological stability issues. We therefore evaluated two different conditions: an acidic environment and the co-incubation in the presence of liver microsomes, to simulate the environments within the stomach and the liver, respectively.

Simple HPLC methods with a short run time were used to visually check the elution of the fragments before and after exposure to 1 M HCl (Figure S8). Since all compounds after 24 h incubation with 1 M HCl produce completely different elution peaks after incubation, all three compounds have little stability in acidic media.

We conducted the metabolic stability assays using commercially available human liver microsomes, which are specific for Phase I processes catalyzed by cytochrome P450 (CYP) monooxygenases and flavin containing monooxygenases (FMO). We selected human instead of murine microsomes because the human is the final species of interest and the results of these metabolic studies can give us an inference of the behavior in our mouse experiments.

The metabolic stability results are summarized in Table 6. The stability of the compounds decreased exponentially with > 40 % compound remaining after 24 h, with similar half-life values ranging from 2.2 – 3.8 h. The intrinsic clearance of the compounds was low and intermediate ranging from 7.5 to 13.3 μL/min/mg.[29]

Table 6. Metabolic stability in human microsomes

Compound	$t_{1/2}$ **(h)**	k **(min^{-1})**	CL_{int} **(μL min^{-1} mg^{-1})**
Fc-CH_2-OXA	3.8	0.003	7.5
Rc-CH_2-OXA	2.2	0.0053	13.3
Ph-CH_2-OXA	2.4	0.0048	12
OXA	3.1	0.0037	9.3

From the values of intrinsic clearance in Table 6, according to McNaney *et al.*, Fc-CH_2-OXA could be categorized as “low” clearance, while Rc-CH_2-OXA, Ph-CH_2-OXA and OXA would be categorized as “intermediate”.[30, 31]

The elution peaks showed (Figure S9, S10 and S11) for Fc-CH_2-OXA, Rc-CH_2-OXA and Ph-CH_2-OXA that only the Ph-CH_2-OXA derivative remained unchanged in an acceptable 56 % after 24 h of incubation in the presence of microsomes, what indicates that the Ph-CH_2-OXA derivative was more resistant to microsomal oxidation, hydroxylation and reduction compared to its metallocenyl analogues, Fc-CH_2-OXA and Rc-CH_2-OXA.

We previously reported[23] excellent *in vivo* efficacy in the *S. mansoni* murine model at 100 mg/kg. At that time, the stability of the compounds was yet unknown. Based on the stability results we obtained, it is entirely possible to attribute some activity of the derivatives to OXA itself, in addition to the derivatives’ own bioactivity. Furthermore, we could infer that the factors of poor metabolic stability, solubility and permeability of the compound to the membrane contributed to the poor *in vivo* results. In order to have a better idea of the permeability of Ph-CH_2-OXA (deemed the most stable candidate *via* stability testing), we proceeded to calculate the MW, logP value, number of Hydrogen bonds donors and Hydrogen bonds acceptors, using the software Molinspiration[32] to estimate its theoretical solubility and membrane permeability. These values gave us a rational basis for selecting a compound for formulation studies aimed at improving bioavailability. Traditionally, therapeutics have been small molecules that fall within the Lipinski's rule of five[33] (i.e., a molecule with a molecular mass ≤ 500 Da, ≤ 5 hydrogen bond donors, ≤ 10 hydrogen bond acceptors, and an octanol–water partition coefficient log P ≤ 5). Molecules violating more than one of these rules may experiment limited bioavailability. Ph-CH_2-OXA has a molecular mass of 369 Da, 6 H-bond acceptors, 2 H-bond donors, and a calculated logP value of 4.26 with 7 rotatable bonds, which were well within the parameters of being an ideally permeable small molecule (Table S2).

It is important to note that it is solubility, permeability and metabolic stability, collectively that have a bearing on the bioavailability of oral drugs. Ph-CH_2-OXA was active *in vitro*, and the *in silico* studies predicted as well a very promising interaction with the parasite's active site on both evaluated species. Additionally, since Ph-CH_2-OXA was metabolically the most stable compound and with predicted acceptable permeability according to the Lipinski's criteria, we proceeded with Ph-CH_2-OXA for further nanoencapsulation formulation studies on the hypothesis that the nanoencapsulated compound would have increased overall solubility and reduced degradation within the acidic environment of the stomach, a new panorama, which would allow better delivery of the compound to its parasitic target.

Lipid Nanocapsules loaded with Ph-CH_2-OXA

Lipid nanocapsules (LNC) are the vector of choice to encapsulate lipophilic molecules.[34] Indeed, LNC present an oily core formed of medium-chain triglycerides covered by a membrane made from a mixture of lecithin and a PEGylated surfactant [34] (Figure 3): this core is able to encapsulate various lipophilic compounds and LNC have already been intensively used for *in vivo* administration of ferrocifens.[35-38]

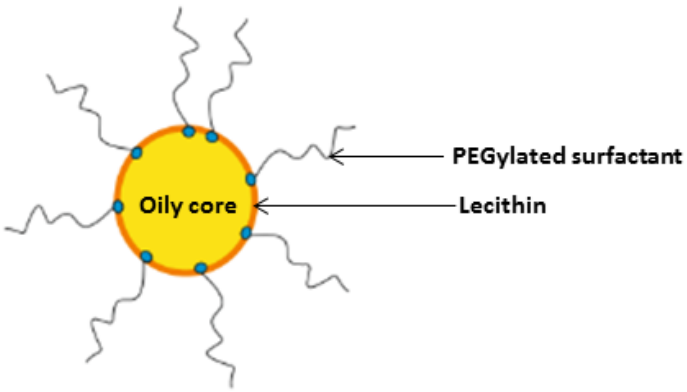

Figure 3. Schematic representation of LNC.

Ph-CH_2-OXA was encapsulated at a concentration of 32.35 mg per mL of LNC, representing a drug loading of 4.35 % w/w. The physico-chemical parameters (characterized by Dynamic Light Scattering), of blank LNC and Ph-CH_2-OXA loaded LNC were the same: diameters of approximately 50 nm, a pdi value below 0.2, which demonstrates a monodispersed population of nanoobjects, and a zeta potential close to neutrality as shown in Table 7.

Table 7. Physico-chemical parameters characterized by DLS of empty LNC (blank) and Ph-CH_2-OXA loaded LNC

Sample	Diameter (nm)	pdi	Zeta potential (mV)
Blank LNC	57.4 ± 0.9	0.07 ± 0.02	-3.9 ± 0.7
Ph-CH_2-OXA LNC	53.0 ± 0.5	0.04 ± 0.02	-3.1 ± 0.1

pdi: Polydispersity index

The *in vivo* activity of the drug loaded nanocapsules was evaluated in mice harboring a 21-day *S. mansoni* infection but this improvement in formulation was not translated into a raise of the activity, as summarized in Table 2. The low activity could be the result of a slow or even an absence of drug release, and/or a limited pathogen LNC internalization. In a study instigating the release of different dyes from LNC to a lipophilic compartment mimicking the cells lipid membrane, lipophilic indocarbocyanine dyes were reported to stay entrapped in the surfactant shell of the LNC and no transfer was observed.[39] In a similar paper, studying the transfer *in vivo* of different dyes from LNC to different lipophilic acceptors, the absence of release of lipophilic indocarbocyanine from LNC was confirmed.[40] The Ph-CH_2-OXA being similar in terms of hydrophobicity, the same behavior could be hypothesized and explain the lack of increase of activity of the LNC in comparison to the pure compound.

Conclusion

In this study, we followed up on three OXA analogues that had shown promising antischistosomal activity. The computational models forecast that the ferrocene- and benzene-containing analogues sample far more near attack configurations with the target sulfotransferase than the parent compound (OXA) for *S. mansoni.* On the contrary, in *S. haematobium*, only the *S*-enantiomer of Ph-CH_2-OXA shows the most significant improvement over OXA and could be active against this species. *In vitro,* the derivatives showed improved activity compared to OXA, against adult worms of all three species evaluated (*S. mansoni, S. haematobium* and *S. japonicum)* and against juvenile *S. mansoni*. When considering the *in vivo* studies instead, we evidenced a lack of activity for all three derivatives against juvenile *S. mansoni* and adult *S. haematobium.* We found that all three compounds were only slightly cleared in the *in vitro* liver model but were poorly stable within an acidic environment. This is likely the reason as to why the promising *in vitro* results did not translate to *in vivo* activity. We further evaluated if the lipid nanoencapsulation of the lead compound (Ph-CH_2-OXA) could overcome this limitation, but unfortunately the formulated compound was also inactive. Since the stability and not the activity on the target seems to be the main limitation of these molecules, further steps should include additional strategies for improved drug formulation, to find out if an enhanced bioavailability can overcome the loss of *in vivo* activity.

EXPERIMENTAL SECTION

^{1}H and ^{13}C NMR spectra

All chemicals were either commercially available or were prepared following standard literature procedures. Solvents were used as received or distilled using standard procedures. All preparations were carried out using standard Schlenk techniques.

^{1}H and ^{13}C NMR spectra were recorded in deuterated solvents on Bruker 400 or 500 MHz spectrometer at room temperature. The chemical shifts, δ, are reported in ppm (parts per million).

The residual solvent peaks have been used as internal references. The abbreviations for the peak multiplicities are as follows: s (singlet), d (doublet), t (triplet), m (multiplet). ESI mass spectrometry was performed using a LTQ-Orbitrap XL from Thermo Scientific. Elemental analysis was performed at Science Centre, London Metropolitan University using Thermo Fisher (Carlo Erba) Flash 2000 Elemental Analyser, configured for % CHN. The scanned spectra of the compounds are available in the SI.

OXA-Derivatives preparation

The OXA derivatives were prepared starting from the parent compound oxamniquine (Pfizer) as described previously.[23] The analytical data matched that previously reported and is available in the SI for further reference.[23]

Animals and parasites

All animal experiments were conducted at the Swiss Tropical and Public Health Institute (Swiss TPH) and authorized by the animal welfare office Kanton Basel Stadt, Switzerland (Authorization no. 2070).

NMRI female mice were purchased from Charles River (Sulzfeld, Germany) at the age of three weeks and were left without intervention for one week of acclimatization. Mice were infected with a subcutaneous infection of around 100 cercariae in the back of the neck, following the procedure described by Lombardo *et al*. [41]

For the *S. haematobium* chronic infection, one-month old LVG hamsters (Charles River, NY) were provided by the National Institutes of Health (NIH)–National Institute of Allergy and Infectious Diseases (NIAID) Schistosomiasis Resource Center (SRC) for distribution by the Biomedical Research Institute in Rockville, USA, which were pre-infected with 350 *S. haematobium* cercariae. The animals were kept in the animal facility with humidity and light control (50 % - 12/12) for three months.

Swiss Webster mice infected with *S. japonicum* (Philippine strain) were also obtained from NIH NIAID SRC for our *in vitro* studies.

***In vitro* studies**

Adult *S. mansoni, S. haematobium* and *S. japonicum* worms were collected by dissection from the mesenteric veins. Until use (within 24 h after dissection) and during the experiments, the worms were kept in the incubator by 37°C and 5% CO_2 and the culture medium consisted of RPMI 1640 (Gibco - Thermofisher, Waltham, MA USA) supplemented with 1% penicillin/streptomycin (BioConcept, Allschwil, Switzerland) and 5% Fetal Calf Serum (FCS) (BioConcept). The control groups consisted of culture medium spiked with dimethyl sulfoxide (DMSO) at a concentration of 1% or 0.5%, equivalent to the content of DMSO present in the wells of worms treated with the highest drug concentration for that assay. The concentrations evaluated were 100, 50, 25, 12.5 and 6.25 µM. The studies on *S. mansoni* and *S. japonicum* were performed as duplicates and repeated once, while the studies on *S. haematobium* were performed in duplicates. Every study condition included at least three worms.

We further evaluated the effect of the addition of albumin (AlbuMAX II, Gibco) to the culture medium to investigate if the activity of the derivatives was different. For this we set the same assay design as described before and added 45 g/l albumin to the culture medium, corresponding to the content of albumin within the range of human plasma.[42] We performed the study with medium containing albumin on adult *S. mansoni* (duplicate and repeated once), and on adult *S. haematobium* (on duplicate). To assign a score to the viability, we used a previously described method[43] scoring motility, viability, and morphological alterations using a bright field inverted microscope (Carl Zeiss Oberkochen, Germany, magnification ×4 and ×10).

***S. mansoni juvenile* worms for *in vitro* studies**

28 days after infection, mice were euthanized and juvenile worms were obtained by blood perfusion. The perfusion solution consisted of 8.5 g/L NaCl, 7.5 g/L Na-citrate in distilled water. Parasites were in different stages of development, as reported somewhere else.[44] All juvenile worms were kept in culture medium as described before for adult *S. mansoni* until use within 24 h. To test the activity of the derivatives against the juvenile stages, we incubated the worms with a 100 µM concentration of each of the derivatives in duplicates and at least two worms per well. Duplicates of 100 µM OXA and 1 % DMSO served as control conditions.

Calculation of IC_{50} values

CompuSyn 1.0 (ComboSyn Inc, 2007) was used to calculate the IC_{50} values of each of the derivatives after an incubation period of 72 h. The following equation was used to normalize the scores of the treated worms to the controls:

$$\text{Effect} = 1 - \frac{\text{average score treatment}}{\text{average score control}}$$

Statistical analysis

All statistics were performed using RStudio version 3.5.1[45]. For evaluating significance in the *in vivo* studies we applied the non-parametric Kruskall Wallis test for multiple comparisons, and the Dunn test with Bonferronni correction for individual differences. Significance was defined as an adjusted p value < 0.05. To evaluate if there was difference in gender susceptibility we applied the binomial test.

Drug suspension for oral administration

The derivatives were administered to the animals in form of an oral suspension. The compounds were first dissolved in DMSO (Sigma-Aldrich, Buchs, Switzerland) corresponding to 10% of the total volume, and then a mixture of Tween 80 and ethanol in a proportion of 70:30 was added, also corresponding to 10% of the final volume. The remaining 80% of the volume consisted of distilled water, which was added under stirring by small aliquots.

In vivo* activity on juvenile *S. mansoni

21 days after infection, mice were treated orally with each of the derivatives and the nanocapsules loaded with Ph-CH_2-OXA at a concentration of 200 mg/kg. The control group consisted of four mice which were infected on the same day and under the same conditions as the treatment arm, but were not treated avoiding additional stress, in accordance to animal welfare regulations. Four weeks after treatment (seven weeks after infection), when the worms reached the adult stage of development, the mice were euthanized with CO_2, dissected and the remaining alive worms were picked out from the mesenteric veins and liver, sexed and counted.

In vivo* activity on adult *S. haematobium

The hamsters harboring an adult infection were treated with a dose of 200 mg/kg of the compounds. Three weeks after treatment, the hamsters were euthanized with CO_2, dissected and the worms were picked out from the mesenteric veins and liver, sexed and counted. The control group consisted of four untreated hamsters.

Computational studies

Classical molecular dynamics simulations were performed of the target proteins, i.e. the sulfotransferase of *S. mansoni* (SmSULT) and of *S. haematobium* (ShSULT), in complex with OXA, Fc-CH_2-OXA and Ph-CH_2-OXA. Since the two enantiomers of OXA show different activities against schistosomes,[12, 46] we performed separate simulations for both enantiomeric forms of all molecules.

To develop force field parameters for the drugs, the geometry of all compounds was optimized in the gas phase with the Gaussian 16 software package,[47] using DFT with B3LYP functional and a 6-31+G* basis set for non-metallic atoms and LANL2DZ pseudopotential for the iron atom. The initial geometries were taken from crystallized *S*-OXA complexed to SmSULT (PDB: 4MUB[11]). Hess *et al.* crystallized in 2017 the *R*-enantiomer of Fc-CO-OXA[23] and we used this structure as a starting point

for all *R*-isomers. The electrostatic potential was computed with the same functional and basis set in order to estimate the effective atomic point charges through RESP fitting.[48]

Classical molecular dynamics simulations were performed using Amber16.[49] The protein was modelled using the FF14SB force field and the Generalized Amber Force Field 2 (*gaff2*) was used as a base for the ligands. The ferrocenyl group was modelled using the force field published by Doman *et al.*[50] To estimate the missing dihedral parameters between the ferrocenyl group and the rest of the molecule, we scanned the angles of interest and performed DFT single point energy calculations for all angles, using the same functional, basis set and pseudopotential as for the geometry optimization. We then used the software *paramfit* from AmberTools16[49] to estimate the parameters. To prevent clashes between nuclei during the rotation, we performed these computations on subsystems containing solely atoms that are relevant for these parameters (e.g. Fc-CH_2-NH_2, Fc-CH_2-N-$(CH_3)_2$, Fc-CO-NH_2 and Fc-CO-N-$(CH_3)_2$). All parameters determined in this way accurately reproduce the corresponding *ab initio* energy profiles (Figure S5).

The crystallographic structures of SmSULT and ShSULT with OXA and the cofactor 3'-phosphoadenosine-5'-phosphate (PAP) served as a starting point for our simulations (PDB: 4MUB and 5TIY,[46] respectively). OXA was replaced by its derivatives through alignment of their shared atomic groups. 3'-phosphoadenosine-5'-phosphosulfate (PAPS), the active version of PAP, was inserted in the same way by minimizing the distance between shared PAP atoms. Missing loops of the protein were added using the ModLoop web server.[51] Using *tleap*, the resulting system was put in an 84 x 84 x 84 $Å^3$ periodic box filled with explicit TIP3P water molecules. Finally, the total charge was neutralized by adding Na^+ counter-ions. The resulting systems consisted of about 50,000 atoms.

Classical trajectories were computed using Amber's CUDA version of the PMEMD program. After minimization, the SHAKE algorithm[52] was used to constrain covalent bonds involving hydrogen

atoms and the system was heated to body temperature (T = 310 K) in two steps using a Langevin thermostat. First, the water molecules were heated to the target temperature while restraining the positions of the ligand and protein during 50 ps with a time step of 1 fs. Then, the restraints were released and the whole system was thermalized in the NPT ensemble for 400 ps, with a time step of 1 fs and a pressure relaxation time of 3 ps. We then performed NPT simulations for 40 ns with a time step of 2 fs to reach an equilibrium state of the system. We finally performed 80 ns NPT production runs that were used for analysis.

The binding free energy of the ligands inside the protein was estimated based on the MD trajectories using two methods available in Amber16: Generalized Born Surface Area (MM/GBSA) and Poisson Boltzmann Surface Area (MM/PBSA).[53]

pH and metabolic stability studies

The stability of the three OXA derivatives was studied by *in vitro* co-incubation with acidic environment. To 200 µL of HPLC grade MeCN in a 1.5 mL Eppendorf, 2 µL of 37 % HCl were added to form a final 0.1 M HCl solution. 10 µL test compound (5 mM in HPLC MeCN) were then added to this acidic solution. For the non-acidic control samples, 10 µL test compound (5 mM in HPLC MeCN) were added to 200 µL of HPLC grade MeCN. The compounds were then incubated for 24 h at 37 °C and assessed at t = 0 h and t = 24 h.

Analytical HPLC measurement was performed using a 1260 Infinity HPLC System (Agilent Technology) comprising: 2 x Agilent G1361 1260 Prep Pump system with Agilent G7115A 1260 DAD WR Detector equipped with an Agilent Pursuit XRs 5C18 (100 Å, C18 5 µm 250 x 4.6 mm) Column. The solvents were acetonitrile (HPLC grade) and purified water (Pacific TII) with flow rate 1 mL/min. Detection was performed at 215 nm, 250 nm, 350 nm, 450 nm, 550 nm and 650 nm with a slit of 4 nm. The flow rate was 1 mL/min and the max pressure was set 200 bar. Run parameters

were as follows: 0 min 85 % acetonitrile (MeCN) 15 % H_2O; 3 mins 85 % MeCN 15 % H_2O; 7 min 100 % MeCN ; 9 min 100 % MeCN , 11 min 85 % MeCN 15 % H_2O.

The metabolic stability of the three OXA derivatives was studied by *in vitro* co-incubation with human liver microsomes. All three compounds were incubated in the presence of NADPH at 37 °C. The protocol was adapted from previous studies:[54, 55] 10 µL of 20 mg/mL microsomes (GIBCO, 50 pooled), 463 µL of PBS (GIBCO, 1x PBS) and 2 µL of 40 mM NADPH (Sigma) were added to 1.5 mL Eppendorf tubes and incubated at 37 °C for 10 min to prime the microsomes. Following this, 10 µL of 50 mM test compound and an additional 15 µL of NADPH were added (1 mM final concentration of test compound in 500 µL total volume). The samples were incubated at 37 °C, and quenched at the desired time points of 1, 4 and 24 h by adding 2 mL of dichloromethane (DCM) or any other organic solvent. 2.5 µL of 5 mM caffeine (TCI Chemicals) in HPLC MeCN as internal standard were added during the quenching process. The mixture was shaken for 10 min to ensure complete extraction. The DCM layer was carefully removed and then evaporated to provide residues that were analyzed by LC-MS (HPLC Waters 2525/Mass Spectrometry Waters ZQ 2000) using a pure acetonitrile-water system with the same column as above. The residues were dissolved in 100 µL HPLC grade acetonitrile. 20 µL from each MeCN residue sample was injected manually using the following run parameters: 3 min 5 % MeCN 95 % H_2O; 13 min 40 % MeCN 60 % H_2O; 14 min 100 % MeCN 0 % H_2O; 20 min 100 % MeCN 0 % H_2O; 23 min 5 % MeCN 95 % H_2O. UV spectra were analyzed and compared at different time points.

By comparing the differences in respective *m/z* values in MS spectra, *m/z* values for the parent compound and OXA could be identified. Semi-quantitative analysis of the ratio of parent compound and different metabolites present in the mixture after incubation with human liver microsomes was achieved by comparing the areas under the respective peaks of different

compounds visible in the UV traces of the LC analysis at 245 nm. To determine the *in vitro* half-life ($t_{1/2}$), the following process was derived from Tan *et al.*[56]

The peak areas of the compounds at different time points are expressed first as a percentage of the internal standard, caffeine.

$$\text{Ratio at timepoint} = \frac{\text{Area under curve of compound}}{\text{Area under curve of internal standard}}$$

Following this, normalized ratios were calculated using the ratio of peak area of the test compounds to caffeine at t = 0 h. Normalised ratios were calculated at each assessed timepoint of t = 1 h, 4 h and 24 h.

$$\text{Normalised ratio} = \frac{\text{Ratio at timepoint} \neq 0}{\text{Ratio at timepoint} = 0}$$

The normalized ratio values are then plotted against incubation time. The $t_{1/2}$ values calculated via analyses methods in GraphPad Prism 8 (nonlinear regression, exponential one phase decay). The degradation rate constant, k was then calculated using the $t_{1/2}$ values (converted from hours to minutes).

The predicted *in vitro* intrinsic clearance values (expressed as µL/min/mg protein) were then calculated as a ratio of the degradation rate constant k (expressed as min^{-1}) and the microsomal protein concentration (mg/µL).

$$\textit{in vitro} \text{ intrinsic clearance values } CL_{int} = \frac{k}{\text{microsomal protein content (0.4 mg/mL protein)}}$$

Ph-CH_2-OXA loaded lipid nanocapsules

Lipid nanocapsules (LNC) were formulated by the phase inversion phase method.[57] Briefly, to prepare blank LNC, Labrafac® (Gattefossé SAS, France, 20.6 % w/w), Lipoid® S 100 (Ludwigshafen, Germany 1.5 % w/w), Kolliphor HS 15 (Florham Park, USA 17 % w/w), NaCl (Sigma-Aldrich, USA 1.3

% w/w) and water (59.6 % w/w) were mixed and homogenized under magnetic stirring at 80 °C. Three cycles of progressive heating and cooling between 90 °C and 50 °C were then performed. During the last cooling cycle, the mixture was diluted by adding 2 °C purified water (28.7 % v/v) in order to induce an irreversible shock and formulate LNC. In order to encapsulate Ph-CH_2-OXA inside the LNC, some slight changes to this protocol have been applied. The Ph-CH_2-OXA (4.35 % w/w) was mixed with Labrafac®, Lipoid® S 100 and ethanol (Fisher, USA) to help solubilization of the molecule in the lipid phase. This mixture was put under agitation at 50 °C until total solubilization of the Ph-CH_2-OXA. The ethanol was then evaporated under argon. Once the ethanol evaporated, Kolliphor HS 15, NaCl and water were added and three heating and cooling cycles were performed as prescribed for formulating blank LNC. During the last cooling cycle, the mixture was diluted by adding 2 °C purified water. Empty LNC and Ph-CH_2-OXA loaded LNC were characterized using Dynamic Light Scattering (DLS) to determine their size, polydispersity index (pdi) and zeta potential.

Ancillary information

Supporting information

Figure S10. Comparison of LCMS trace for Rc-CH_2-OXA before and after incubation for 24 h in liver microsomes

Figure S11. Comparison of LCMS trace for Ph-CH_2-OXA before and after incubation for 24 hours in liver microsomes

Figure S12. ^{1}H NMR spectrum for Fc-CH_2-OXA

Figure S13. ^{1}H NMR spectrum for Rc-CH_2-OXA

Figure S14. ^{1}H NMR spectrum for Ph-CH_2-OXA

Table S2. Molecular properties calculated using Molinspiration (http://molinspiration.com).

* **Corresponding authors**: Email: ursula.roethlisberger@epfl.ch; WWW: https://www.epfl.ch/labs/lcbc/roethlisberger/; Tel. +41 21 693 03 21; jennifer.keiser@unibas.ch; WWW: https://www.swisstph.ch/en/about/mpi/helminth-drug-development/; Tel. +41 76 61 284 82 18; E-mail: gilles.gasser@chimeparistech.psl.eu; WWW: www.gassergroup.com; Tel: +33 1 85 78 41 51.

# Authors have contributed equally to the work.

Conflict of interest

Authors have no competing interests to declare.

Acknowledgements

This work was financially supported by the Swiss National Science Foundation (Grant Sinergia CRSII5_173718) and has received support under the program «Investissements d'Avenir» launched by the French Government and implemented by the ANR with the reference ANR-10-IDEX-0001-02 PSL (G.G.). We are grateful for the loan of analytical instruments by Agilent Technologies and CEA Saclay to Chimie ParisTech. V.B. is grateful to the Swiss excellence scholarships for financial support, scholarship number 2017.0801.

References

1. Colley DG, Bustinduy AL, Secor WE, King CH. Human schistosomiasis. Lancet (London, England). 2014;383(9936):2253-2264.
2. Rotger M, Serra T, de Cárdenas MG, Morey A, Vicente MA. Increasing incidence of imported schistosomiasis in Mallorca, Spain. European Journal of Clinical Microbiology and Infectious Diseases. 2004;23(11):855-856.
3. Berry A, Moné H, Iriart X, Mouahid G, Aboo O, Boissier J, Fillaux J, Cassaing S, Debuisson C, Valentin A, Mitta G, Théron A, Magnaval J-F. Schistosomiasis Haematobium, Corsica, France. Emerging Infectious Diseases. 2014;20(9):1595-1597.
4. Steinmann P, Keiser J, Bos R, Tanner M, Utzinger J. Schistosomiasis and water resources development: systematic review, meta-analysis, and estimates of people at risk. The Lancet Infectious Diseases. 2006;6(7):411-425.
5. Bergquist R, Zhou X-N, Rollinson D, Reinhard-Rupp J, Klohe K. Elimination of schistosomiasis: the tools required. Infect Dis Poverty. 2017;6(1):158-158.
6. Geerts S, Gryseels B. Drug resistance in human helminths: current situation and lessons from livestock. Clinical Microbiology Reviews. 2000;13(2):207-222.
7. Lago EM, Xavier RP, Teixeira TR, Silva LM, da Silva Filho AA, de Moraes J. Antischistosomal agents: state of art and perspectives. Future Medicinal Chemistry. 2017;10(1):89-120.
8. Pica-Mattoccia L, Novi A, Cioli D. Enzymatic basis for the lack of oxamniquine activity in *Schistosoma haematobium* infections. Parasitology Research. 1997;83(7):687-689.
9. Sabah AA, Fletcher C, Webbe G, Doenhoff MJ. Schistosoma mansoni: Chemotherapy of infections of different ages. Experimental Parasitology. 1986;61(3):294-303.
10. Pica-Mattoccia L, Carlini D, Guidi A, Cimica V, Vigorosi F, Cioli D. The schistosome enzyme that activates oxamniquine has the characteristics of a sulfotransferase. Memórias do Instituto Oswaldo Cruz. 2006;101:307-312.
11. Valentim CLL, Cioli D, Chevalier FD, Cao X, Taylor AB, Holloway SP, Pica-Mattoccia L, Guidi A, Basso A, Tsai IJ, Berriman M, Carvalho-Queiroz C, Almeida M, Aguilar H, Frantz DE, Hart PJ, LoVerde PT, Anderson TJC. Genetic and molecular basis of drug resistance and species-specific drug action in Schistosome parasites. Science (New York, NY). 2013;342(6164):1385-1389.
12. Taylor AB, Pica-Mattoccia L, Polcaro CM, Donati E, Cao X, Basso A, Guidi A, Rugel AR, Holloway SP, Anderson TJC, Hart PJ, Cioli D, LoVerde PT. Structural and functional characterization of the enantiomers of the antischistosomal drug oxamniquine. PLOS Neglected Tropical Diseases. 2015;9(10):e0004132.
13. Chevalier FD, Le Clec'h W, Eng N, Rugel AR, Assis RRd, Oliveira G, Holloway SP, Cao X, Hart PJ, LoVerde PT, Anderson TJC. Independent origins of loss-of-function mutations conferring oxamniquine resistance in a Brazilian schistosome population. International Journal for Parasitology. 2016;46(7):417-424.
14. Rugel A, Tarpley RS, Lopez A, Menard T, Guzman MA, Taylor AB, Cao X, Kovalskyy D, Chevalier FD, Anderson TJC, Hart PJ, LoVerde PT, McHardy SF. Design, synthesis, and characterization of novel small molecules as broad range antischistosomal agents. ACS Med Chem Lett. 2018;9(10):967-+.
15. Hillard EA, Vessières A, Jaouen G. Ferrocene functionalized endocrine modulators as anticancer agents. In: Jaouen G, Metzler-Nolte N, editors. Medicinal Organometallic Chemistry. Berlin, Heidelberg: Springer Berlin Heidelberg; 2010. p. 81-117.
16. Biot C, Dive D. Bioorganometallic Chemistry and Malaria. In: Jaouen G, Metzler-Nolte N, editors. Medicinal Organometallic Chemistry. Berlin, Heidelberg: Springer Berlin Heidelberg; 2010. p. 155-193.
17. Gasser G, Metzler-Nolte N. The potential of organometallic complexes in medicinal chemistry. Current Opinion in Chemical Biology. 2012;16(1):84-91.
18. Patra M, Gasser G. The medicinal chemistry of ferrocene and its derivatives. Nature Reviews Chemistry. 2017;1(9):0066.

19. Ong YC, Roy S, Andrews PC, Gasser G. Metal compounds against neglected tropical diseases. Chemical reviews. 2019;119(2):730-796.
20. Dubar F, Egan TJ, Pradines B, Kuter D, Ncokazi KK, Forge D, Paul J-F, Pierrot C, Kalamou H, Khalife J, Buisine E, Rogier C, Vezin H, Forfar I, Slomianny C, Trivelli X, Kapishnikov S, Leiserowitz L, Dive D, Biot C. The antimalarial ferroquine: role of the metal and intramolecular hydrogen bond in activity and resistance. ACS chemical biology. 2011;6(3):275-287.
21. Keiser J, Vargas M, Rubbiani R, Gasser G, Biot C. *In vitro* and *in vivo* antischistosomal activity of ferroquine derivatives. Parasit Vectors. 2014;7:424.
22. Biot C, Taramelli D, Forfar-Bares I, Maciejewski LA, Boyce M, Nowogrocki G, Brocard JS, Basilico N, Olliaro P, Egan TJ. Insights into the mechanism of action of ferroquine. Relationship between physicochemical properties and antiplasmodial activity. Mol Pharm. 2005;2(3):185-193.
23. Hess J, Panic G, Patra M, Mastrobuoni L, Spingler B, Roy S, Keiser J, Gasser G. Ferrocenyl, ruthenocenyl, and benzyl oxamniquine derivatives with cross-species activity against *Schistosoma mansoni* and *Schistosoma haematobium*. ACS infectious diseases. 2017;3(9):645-652.
24. Hess J, Keiser J, Gasser G. Toward organometallic antischistosomal drug candidates. Future Medicinal Chemistry. 2015;7(6):821-830.
25. Buchter V, Hess J, Gasser G, Keiser J. Assessment of tegumental damage to *Schistosoma mansoni* and *S. haematobium* after *in vitro* exposure to ferrocenyl, ruthenocenyl and benzyl derivatives of oxamniquine using scanning electron microscopy. Parasites & Vectors. 2018;11(1):580.
26. Pasche V, Laleu B, Keiser J. Screening a repurposing library, the Medicines for Malaria Venture Stasis Box, against *Schistosoma mansoni*. Parasites & Vectors. 2018;11:298.
27. Olliaro P, Delgado-Romero P, Keiser J. The little we know about the pharmacokinetics and pharmacodynamics of praziquantel (racemate and R-enantiomer). Journal of Antimicrobial Chemotherapy. 2014;69(4):863-870.
28. Keen P. Effect of binding to plasma proteins on the distribution, activity and elimination of drugs. In: Brodie BB, Gillette JR, Ackerman HS, editors. Concepts in Biochemical Pharmacology: Part 1. Berlin, Heidelberg: Springer Berlin Heidelberg; 1971. p. 213-233.
29. Measurement of *in vitro* intrinsic clearance using microsomes [Available from: https://www.cyprotex.com/admepk/in-vitro-metabolism/microsomal-stability. Date accessed [04.06.2020]
30. Colleen A. McNaney DMD, Serhiy Y. Hnatyshyn, Tatyana A. Zvyaga, Jay O. Knipe, James V. Belcastro, and Mark Sanders. An automated liquid chromatography-mass spectrometry process to determine metabolic stability half-life and intrinsic clearance of drug candidates by substrate depletion. ASSAY and Drug Development Technologies. 2008;6(1):121-129.
31. Słoczyńska K, Gunia-Krzyżak A, Koczurkiewicz P, Wójcik-Pszczoła K, Żelaszczyk D, Popiół J, Pękala E. Metabolic stability and its role in the discovery of new chemical entities. 2019;69(3):345.
32. Cheminformatics M. 2001; cited 2020 05.06.2020]. Available from: https://www.molinspiration.com/about.html. Date accessed [05.06]
33. Lipinski CA, Lombardo F, Dominy BW, Feeney PJ. Experimental and computational approaches to estimate solubility and permeability in drug discovery and development settings. Advanced Drug Delivery Reviews. 1997;23(1):3-25.
34. Huynh NT, Passirani C, Saulnier P, Benoit JP. Lipid nanocapsules: a new platform for nanomedicine. Int J Pharm. 2009;379(2):201-209.
35. Laine AL, Huynh NT, Clavreul A, Balzeau J, Bejaud J, Vessieres A, Benoit JP, Eyer J, Passirani C. Brain tumour targeting strategies via coated ferrociphenol lipid nanocapsules. European journal of pharmaceutics and biopharmaceutics : official journal of Arbeitsgemeinschaft fur Pharmazeutische Verfahrenstechnik eV. 2012;81(3):690-693.
36. Allard E, Jarnet D, Vessieres A, Vinchon-Petit S, Jaouen G, Benoit JP, Passirani C. Local delivery of ferrociphenol lipid nanocapsules followed by external radiotherapy as a synergistic treatment against intracranial 9L glioma xenograft. Pharm Res. 2010;27(1):56-64.
37. Karim R, Lepeltier E, Esnault L, Pigeon P, Lemaire L, Lepinoux-Chambaud C, Clere N, Jaouen G, Eyer J, Piel G, Passirani C. Enhanced and preferential internalization of lipid

nanocapsules into human glioblastoma cells: effect of a surface-functionalizing NFL peptide. Nanoscale. 2018;10(28):13485-13501.
38. Laine AL, Adriaenssens E, Vessieres A, Jaouen G, Corbet C, Desruelles E, Pigeon P, Toillon RA, Passirani C. The *in vivo* performance of ferrocenyl tamoxifen lipid nanocapsules in xenografted triple negative breast cancer. Biomaterials. 2013;34(28):6949-6956.
39. Bastiat G, Pritz CO, Roider C, Fouchet F, Lignières E, Jesacher A, Glueckert R, Ritsch-Marte M, Schrott-Fischer A, Saulnier P, Benoit JP. A new tool to ensure the fluorescent dye labeling stability of nanocarriers: a real challenge for fluorescence imaging. Journal of controlled release : official journal of the Controlled Release Society. 2013;170(3):334-342.
40. Simonsson C, Bastiat G, Pitorre M, Klymchenko AS, Béjaud J, Mély Y, Benoit JP. Inter-nanocarrier and nanocarrier-to-cell transfer assays demonstrate the risk of an immediate unloading of dye from labeled lipid nanocapsules. European journal of pharmaceutics and biopharmaceutics : official journal of Arbeitsgemeinschaft fur Pharmazeutische Verfahrenstechnik eV. 2016;98:47-56.
41. Lombardo FC, Pasche V, Panic G, Endriss Y, Keiser J. Life cycle maintenance and drug-sensitivity assays for early drug discovery in *Schistosoma mansoni*. Nature Protocols. 2019:1.
42. Chapter 5: Human Albumin. In: Hemotherapy TMa, editor. 36. 4th ed. S. Karger GmbH, Freiburg: Cross-Sectional Guidelines for Therapy with Blood Components and Plasma Derivatives; 2009. p. 399-407.
43. Keiser J. *In vitro* and *in vivo* trematode models for chemotherapeutic studies. Parasitology. 2010;137(3):589-603.
44. Faust EC, Jones CA. Life history of manson's blood fluke (*Schistosoma mansoni*). III. The Blood Picture in Schistosomiasis Mansoni. Proceedings of the Society for Experimental Biology and Medicine. 1934;31(4):478-479.
45. Team R. RStudio: Integrated Development for R. 3.5.1 ed: RStudio Inc., Boston, MA 2016.
46. Taylor AB, Roberts KM, Cao X, Clark NE, Holloway SP, Donati E, Polcaro CM, Pica-Mattoccia L, Tarpley RS, McHardy SF, Cioli D, LoVerde PT, Fitzpatrick PF, Hart PJ. Structural and enzymatic insights into species-specific resistance to schistosome parasite drug therapy. Journal of Biological Chemistry. 2017;292(27):11154-11164.
47. Frisch MJ, Trucks GW, Schlegel HB, Scuseria GE, Robb MA, Cheeseman JR, Scalmani G, Barone V, Petersson GA, Nakatsuji H, Li X, Caricato M, Marenich AV, Bloino J, Janesko BG, Gomperts R, Mennucci B, Hratchian HP, Ortiz JV, Izmaylov AF, Sonnenberg JL, Williams, Ding F, Lipparini F, Egidi F, Goings J, Peng B, Petrone A, Henderson T, Ranasinghe D, Zakrzewski VG, Gao J, Rega N, Zheng G, Liang W, Hada M, Ehara M, Toyota K, Fukuda R, Hasegawa J, Ishida M, Nakajima T, Honda Y, Kitao O, Nakai H, Vreven T, Throssell K, Montgomery Jr. JA, Peralta JE, Ogliaro F, Bearpark MJ, Heyd JJ, Brothers EN, Kudin KN, Staroverov VN, Keith TA, Kobayashi R, Normand J, Raghavachari K, Rendell AP, Burant JC, Iyengar SS, Tomasi J, Cossi M, Millam JM, Klene M, Adamo C, Cammi R, Ochterski JW, Martin RL, Morokuma K, Farkas O, Foresman JB, Fox DJ. Gaussian 16 Rev. B.01. Wallingford, CT2016.
48. Bayly CI, Cieplak P, Cornell W, Kollman PA. A well-behaved electrostatic potential based method using charge restraints for deriving atomic charges: the RESP model. The Journal of Physical Chemistry. 1993;97(40):10269-10280.
49. D.A. Case RMB, D.S. Cerutti, T.E. Cheatham, III, T.A. Darden, R.E. Duke, T.J. Giese, H. Gohlke, A.W. Goetz, N. Homeyer, S. Izadi, P. Janowski, J. Kaus, A. Kovalenko, T.S. Lee, S. LeGrand, P. Li, C. Lin, T. Luchko, R. Luo, B. Madej, D. Mermelstein, K.M. Merz, G. Monard, H. Nguyen, H.T. Nguyen, I. Omelyan, A. Onufriev, D.R. Roe, A. Roitberg, C. Sagui, C.L. Simmerling, W.M. Botello-Smith, J. Swails, R.C. Walker, J. Wang, R.M. Wolf, X. Wu, L. Xiao and P.A. Kollman AMBER 2016. University of California, San Francisco. 2016.
50. Doman TN, Landis CR, Bosnich B. Molecular mechanics force fields for linear metallocenes. Journal of the American Chemical Society. 1992;114(18):7264-7272.
51. Fiser A, Do RK, Sali A. Modeling of loops in protein structures. Protein science : a publication of the Protein Society. 2000;9(9):1753-1773.
52. Ryckaert J-P, Ciccotti G, Berendsen HJC. Numerical integration of the cartesian equations of motion of a system with constraints: molecular dynamics of n-alkanes. Journal of Computational Physics. 1977;23(3):327-341.

53. Miller BR, McGee TD, Swails JM, Homeyer N, Gohlke H, Roitberg AE. MMPBSA.py: an efficient program for end-state free energy calculations. Journal of Chemical Theory and Computation. 2012;8(9):3314-3321.
54. Patra M, Ingram K, Leonidova A, Pierroz V, Ferrari S, Robertson MN, Todd MH, Keiser J, Gasser G. *In vitro* metabolic profile and *in vivo* antischistosomal activity studies of (η6-Praziquantel)Cr(CO)3 derivatives. Journal of Medicinal Chemistry. 2013;56(22):9192-9198.
55. Keller S, Ong YC, Lin Y, Cariou K, Gasser G. A tutorial for the assessment of the stability of organometallic complexes in biological media. Journal of Organometallic Chemistry. 2020;906:121059.
56. Tan J, Sivaram H, Huynh HV. Gold(I) bis(N-heterocyclic carbene) complexes: metabolic stability, *in vitro* inhibition, and genotoxicity. 2018;32(8):e4441.
57. Heurtault B, Saulnier P, Pech B, Proust J-E, Benoit J-P. A novel phase inversion-based process for the preparation of lipid nanocarriers. Pharmaceutical Research. 2002;19(6):875-880.

TOC Graphic (TIFF format)